Pedosphere **36**(2): 484–496, 2026
doi: 10.1016/j.pedsph.2024.10.003
ISSN 1002-0160/CN 32-1315/P

Published by Elsevier B.V. and Science Press

PEDOSPHERE

www.elsevier.com/locate/pedosphere

Mineral-associated organic carbon promotes phosphorus accumulation in a long-term fertilized black soil

Naiyu ZHANG[1,2], Xiuzhi ZHANG[3], Yanhua CHEN[1], Lehlogonolo Abner MATELELE[1], Ping ZHU[3], Hongfang LIU[1], Xianmei ZHANG[1], Hongjun GAO[3], Gu FENG[2], Chang PENG[3] and Shuxiang ZHANG[1,*]

[1]*Key Laboratory of Arable Land Quality Monitoring and Evaluation, Ministry of Agriculture and Rural Affairs/State Key Laboratory of Efficient Utilization of Arid and Semi-arid Arable Land in Northern China, Institute of Agricultural Resources and Regional Planning, Chinese Academy of Agricultural Sciences (CAAS), Beijing 100081 (China)*
[2]*College of Resources and Environmental Sciences, China Agricultural University, Beijing 100193 (China)*
[3]*Institute of Agricultural Resources and Environment, Jilin Academy of Agricultural Sciences, Changchun 130033 (China)*

(Received April 2, 2024; revised August 19, 2024; accepted September 29, 2024)

ABSTRACT

Soil phosphorus (P) pools are intimately connected to organic carbon (OC), especially mineral-associated OC (MAOC). However, the relationships between MAOC fractions and P fractions and their responses to fertilization remain unclear. In a long-term field experiment established on a black soil (Mollisol) in Gongzhuling, Jilin Province, Northeast China, in 1989, topsoils with no fertilizer (control, CK), conventional application of chemical fertilizer (CF), and chemical fertilizer combined with straw addition (CFS) were sampled in 2010 (21 years) and 2018 (29 years), and organo-mineral complexes ($<$ 20 μm) were separated and analyzed. Compared to CK, the CF treatment resulted in soil acidification, increasing the content of the MAOC fraction bound to minerals by weak linkages in complexes. The CFS treatment maintained soil pH at 7.84 in 2010 and 7.53 in 2018, with significantly higher contents of four MAOC fractions, remaining water-soluble OC, OC bound by cations, OC encapsulated by resistant carbonate, and insoluble OC (humin), than those in the CF treatment. Fertilization application increased total P content in the organo-mineral complexes, with similar total P content between the CF and CFS treatments. Chemical fertilizer mainly increased highly labile inorganic P (P_i) extracted by resin strips + deionized water, $NaHCO_3$, and NaOH, as well as organic P (P_o) extracted by $NaHCO_3$, and straw addition mainly increased moderately labile P_i extracted by dilute HCl. Correlation analysis showed that the dominant MAOC fractions had positive relationships with the increased P fractions. X-ray absorption near-edge structure spectroscopy further identified that the CF treatment increased the proportion of $AlPO_4$, suggesting that MAOC promoted the retention of labile P *via* association with aluminum (Al) under weakly acidic conditions. The CFS treatment increased the proportion of $Ca_3(PO_4)_2$ and $Ca_5(PO_4)_3OH$; moreover, it also increased the maximum P sorption capacity of the organo-mineral complexes, suggesting that MAOC enhanced P sorption *via* association with calcium (Ca) under weakly alkaline conditions and that adsorbed P would transform into more stable Ca-associated P. Our findings demonstrated that MAOC promoted P accumulation *via* association with different P fractions, and these processes were mineral- and pH-dependent.

Key Words: chemical fertilizer, maximum P sorption capacity, Mollisol, organo-mineral complexes, P fraction, P species, straw addition

Citation: Zhang N Y, Zhang X Z, Chen Y H, Matelele L A, Zhu P, Liu H F, Zhang X M, Gao H J, Feng G, Peng C, Zhang S X. 2026. Mineral-associated organic carbon promotes phosphorus accumulation in a long-term fertilized black soil. *Pedosphere*. **36**(2): 484–496.

INTRODUCTION

Phosphorus (P) is necessary for crop growth. Human survival depends on a large input of P fertilizer for crop production (Cordell *et al*., 2009; Mogollón *et al*., 2018). However, over the past decades, the fixation of P in soil has led to its accumulation (MacDonald *et al*., 2011), as well as the environmental problem that accumulated P tends to enter waterbodies, causing eutrophication (Wu *et al*., 2022). As the front end of the P flow chain, the transformation and availability of soil P pools are crucial for the back end, such as plant uptake and environmental behavior (Shen *et al*., 2019). Therefore, understanding the characteristics of soil P pools and their influencing factors is essential for soil P management.

Soil P pools are mainly influenced by fertilization. Chemical fertilizer application mainly increases labile/moderately labile P based on chemical fractionation (Audette *et al*., 2016; Liu *et al*., 2017). Compared to chemical fertilizer alone, straw addition can promote labile P and decrease stable P (Cao *et al*., 2022; Zhang Y J *et al*., 2022). Straw addition enhances the microbial transformation of soil P and thus promotes P availability in short order (Cao *et al*., 2022). In the long run, differences in soil P pools between treatments with organic fertilizers and chemical fertilizers alone may be explained by different soil properties such as pH, organic matter (OM), and iron (Fe)/aluminum (Al) (hydro)oxides (Yan *et al*., 2018; Ando *et al*., 2022; Zhang Y J *et al*., 2022).

*Corresponding author. E-mail: zhangshuxiang@caas.cn.

Soil OM is crucial for soil structure and function, especially in regulating soil P (Jindo *et al*., 2023). Generally, soil OM and P contents exhibit positive correlations or similar spatial distributions in bulk soils (de Oliveira *et al*., 2022), soil aggregates (Tian *et al*., 2022), or soil density fractions (Takamoto *et al*., 2021). According to previous reports, the maximum P sorption capacity ($Q_{\rm m}$) of soils increases with increasing OM (Kang *et al*., 2009). Yang *et al*. (2019) demonstrated that increasing OM in a black soil by adding humic acid also increased the $Q_{\rm m}$. In another study, it was found that the $Q_{\rm m}$ in peat soils increased with the application of Fe-OM associations and was much higher than that with the application of Fe alone (Yang *et al*., 2022).

Soil OM regulates P by many mechanisms, such as competition, complexation, and cation bridge (Fink *et al*., 2016; Jindo *et al*., 2023). Among them, cation bridges are widely present in soil and conducive to P accumulation (Li *et al*., 2021; Takamoto *et al*., 2021). Typically, humus-like OM associated with calcium (Ca) can bind P to form ternary complexes of OM-Ca-P, delaying the conversion of amorphous Ca-associated P to the more stable state (Sindelar *et al*., 2015; Ge *et al*., 2020). Similarly, OM can enhance Fe/Al (hydro)oxides to bind P and occur as OM-Fe/Al-P in soil (Fink *et al*., 2016; Takamoto *et al*., 2021; Jindo *et al*., 2023). The sorption or accumulation of soil P depends on the characteristics (such as solubility, stability, and humification degree) of OM (Yang *et al*., 2019; Li *et al*., 2021, 2022). Although many reports have assessed quantitative relationships between soil OM and P sorption or accumulation, the effects of OM fractions with different characteristics on soil P pools, as well as their responses to fertilization practices, remain unclear.

Organic carbon (OC) is the skeleton of soil OM, and it is estimated that more than half of OC is associated with soil minerals (Georgiou *et al*., 2022). Organo-mineral complexes, as the core of mineral-associated OC (MAOC) storage and active components of soil, are formed by the binding of OC and minerals (Schmidt *et al*., 2011; Zheng *et al*., 2023). Based on chemical sequential extractions, both MAOC and P pools can be separated into different fractions with specific characteristics (Tiessen and Moir, 1993; Lopez-Sangil and Rovira, 2013), which contribute to elucidating the relationship and mechanisms between MAOC and P fractions in the organo-mineral complexes.

We investigated the impacts of different fertilization practices on the P and MAOC fractions in the organo-mineral complexes, as well as the relationships between the P fractions and the MAOC fractions. We hypothesized that: i) fertilization would influence the P and MAOC fractions in the organo-mineral complexes, ii) there would be strongly positive correlations between different P fractions and specific MAOC fractions, and iii) MAOC association with different soil minerals would contribute to the accumulation of the corresponding P fractions under different fertilization practices. These results might provide fresh insight into how soil OM regulates P and guide future P management.

MATERIALS AND METHODS

Experimental design

A long-term field experiment was conducted in Gongzhuling, Jilin Province, Northeast China, in 1989 (124.809° E, 43.506° N). The experimental site had a continental monsoon climate in the mid-temperate humid zone. The area has an average annual precipitation of 525 mm (ranging from 450 to 650 mm) and an average annual temperature of 4.5 °C (ranging from −35 to 34 °C). The soil in the study area is classified as a black soil in Chinese Soil Taxonomy (Mollisol in US Department of Agriculture Soil Taxonomy and Phaeozem in World Reference Base). The initial topsoil (0–20 cm) had a pH of 7.6, soil OM of 21.9 g kg^{-1}, $CaCO_3$ of 14.6 g kg^{-1}, total nitrogen (N) of 1.4 g kg^{-1}, total P of 0.61 g kg^{-1}, total potassium (K) of 18.4 g kg^{-1}, available N (alkali hydrolyzable N) of 114 mg kg^{-1}, Olsen-P of 11.8 mg kg^{-1}, and available K of 158.3 mg kg^{-1}. The cropping system was a maize monoculture with one crop per year. The fertilization treatments were performed in a completely randomized block design with three replications. Tillage was carried out using a mechanical rotary plough after harvest each year. More detailed information about the experiment was introduced in previous reports (Cui *et al*., 2022; Zhang N Y *et al*., 2022). After the maize harvest in October each year, five cores of the topsoil (0–20 cm) were randomly drilled in each plot based on an S pattern and mixed into a single sample. After removing the rocks and thick roots, the soil samples were air-dried, sieved through a 2-mm sieve, and finally archived in plastic bottles.

We selected soil samples archived in 2010 and 2018 from three typical fertilization practices: no fertilizer (control, CK), conventional application of chemical fertilizer (CF), and chemical fertilizer combined with straw addition (CFS). The chemical fertilizers applied were urea for N, triple superphosphate for P, and potassium chloride for K. For the CF treatment, the chemical N-P-K fertilizer rates were 165-36-68.5 kg ha^{-1}. For the CFS treatment, the chemical N-P-K fertilizer rates were 112-36-68.5 kg ha^{-1}, with the addition of all maize straw containing 7 500 kg ha^{-1} dry mass and 53-6-58 kg ha^{-1} of N-P-K. Straw was returned to the field by crushing and mulching. We assumed that the additional 6 kg P ha^{-1} in straw would contribute less to P variation per unit mass of soil. Furthermore, we would focus on the synergistic mechanism of SOC storage and P accumulation and the contributing factors. Therefore, this experiment is still valuable despite the limitation of inconsistent nutrient inputs.

Soil organo-mineral complex separation and property determination

In order not to introduce chemical reagents, the organo-mineral complexes in soil were separated and collected using a modified physical fractionation procedure according to previous reports (Lopez-Sangil and Rovira, 2013; Sayer *et al.*, 2019). Soil samples (30 g) were weighed into 250-mL triangular flasks with a dozen small glass marbles and 100-mL distilled water. The flasks were shaken for 60 min (20 r min^{-1}). After removing the glass marbles, the soil-water mixtures were dispersed by ultrasound for 10 min, with the samples immersed in an ice-water bath to prevent heating. The dispersed mixtures were transferred to a 1 000-mL glass cylinder, stirred up and down with a stirrer for 30 strokes, and left to stand. A sedimentation process was used instead of passing through a 20-μm sieve. According to Stokes' Law, < 20 μm organo-mineral complexes were obtained by aspirating 10 cm of the upper layer of the suspension after 4 min 15 s of standing at 25 °C, and this was repeated until all the suspension was depleted. The suspension collected was dried at 60 °C and sieved (0.15 mm) for subsequent analyses. The soil pH, the same as the pH of the organo-mineral complexes, was measured at a soil/water ratio of 1:2.5 (weight/volume). Selected chemical properties of the organo-mineral complexes were determined as follows. Total P was determined using the NaOH melting method (Lu, 2000), amorphous Fe and Al (Fe_o and Al_o, respectively) were extracted using 0.2 mol L^{-1} ammonium oxalate at pH 3 (McKeague and Day, 1966), organically complexed Fe and Al (Fe_p and Al_p, respectively) were extracted using 0.1 mol L^{-1} $Na_4P_2O_7$ at pH 10 (Mikutta *et al.*, 2006), and exchangeable Ca and magnesium (Mg) (Ca_{ex} and Mg_{ex}, respectively) were extracted with 1 mol L^{-1} ammonium acetate (Lu, 2000). The concentrations of Fe, Al, Ca, and Mg in the extract solutions were measured by an inductively coupled plasma optical emission spectrometer (Varian 715-ES, Agilent Technologies, USA).

Sequential fractionation of MAOC in the organo-mineral complexes

The MAOC fractions in soil organo-mineral complexes were determined by chemical sequential fractionation. Briefly, 1 g organo-mineral complexes was weighed into a 50-mL centrifuge tube, and 35 mL various chemical extractants were added sequentially and individually in the order of: i) 0.5 mol L^{-1} K_2SO_4, ii) 0.1 mol L^{-1} $Na_2B_4O_7$ (pH 9.7), iii) 0.1 mol L^{-1} $Na_4P_2O_7$ (pH 10.2), iv) 0.1 mol L^{-1} NaOH (pH 12), v) 0.33 mol L^{-1} H_2SO_4 + 0.1 mol L^{-1} NaOH, vi) 0.1 mol L^{-1} $Na_2S_2O_4$ (pH 8) + 0.1 mol L^{-1} NaOH, and vii) 8 mol L^{-1} HF + 0.1 mol L^{-1} NaOH to obtain MAOC fractions, the remaining water-soluble OC (K_2SO_4-OC), OC bound to minerals by weak linkages ($Na_2B_4O_7$-OC), OC bound by cations ($Na_4P_2O_7$-OC), OC extracted in massive quantities by NaOH (NaOH-OC), OC encapsulated by resistant carbonate (H_2SO_4-OC), OC stabilized by Fe (hydro)oxides ($Na_2S_2O_4$-OC), and OC bound to minerals by strong bonds (HF-OC), respectively. Each step of the extraction was repeated at least twice. The OC in the final soil residues was insoluble compounds (humin). The detailed MAOC fractionation procedure was described in Lopez-Sangil and Rovira (2013). The extracts collected and final soil residues were digested using 0.17 mol L^{-1} $K_2Cr_2O_7$ and concentrated sulfuric acid, followed by colorimetric determination of OC content at 600 nm (Soon and Abboud, 1991). The sum of all MAOC fractions was treated as the total MAOC in the organo-mineral complexes. In this study, HF-OC was not detected.

Sequential fractionation of P in the organo-mineral complexes

The separation of the organo-mineral complexes was carried out by a physical method without the introduction of chemical reagents, which may have had fewer impacts on the inorganic (P_i) and organic P (P_o) pools. Therefore, the possible impacts were ignored. Nine P fractions were extracted and quantified by chemical sequential fractionation following Tiessen and Moir (1993) (Table SI, see Supplementary Material for Table SI). Briefly, 0.5 g of organo-mineral complexes was added to a 50-mL centrifuge tube and extracted sequentially by resin strips + deionized water (resin-P_i), 0.5 mol L^{-1} $NaHCO_3$ at pH 8.5 ($NaHCO_3$-P_i/P_o), 0.1 mol L^{-1} NaOH (NaOH-P_i/P_o), 1 mol L^{-1} dilute HCl (Dil. HCl-P_i), 12 mol L^{-1} concentrated HCl (Con. HCl-P_i/P_o), and 30% H_2O_2 + 18 mol L^{-1} H_2SO_4 (residual P). The concentrations of P_i in the extracts collected were analyzed by spectrophotometry (Murphy and Riley, 1962). The extracts of $NaHCO_3$, NaOH, and Con. HCl were digested with H_2SO_4-$(NH_4)_2S_2O_8$ solution in an autoclave to measure total P content. The P_o was calculated as the difference between total P and P_i.

Identification of P species in soil organo-mineral complexes by X-ray absorption near-edge structure (XANES) spectroscopy

The possible P species in the organo-mineral complexes were identified by P K-edge XANES spectroscopy at Beijing Synchrotron Radiation Facility, China. Seven references for P species were selected according to Liu *et al.* (2019), including $CaHPO_4$, $Ca(H_2PO_4)_2$, $Ca_3(PO_4)_2$, $Ca_5(PO_4)_3OH$, $FePO_4$, $AlPO_4$, and inositol hexaphosphate. In black soils, Ca is abundant and a potential phosphate adsorbent, so we chose more references for Ca-associated P compounds. The spectra of P references were collected in total electron yield mode, while samples of organic-mineral complexes were collected in partial fluorescence yield mode. The spectral data collected were normalized and calibrated for background and baseline using Athena software (version 0.9.26, Inc., Boston, USA), and linear combination fitting based on the spectra of references was carried out to identify possible P species in the organo-mineral complexes. The energy range of the linear combination fitting was 2 140–2 180 eV. The combination with the highest number of P references was selected as the possible P species.

Organo-mineral complex P sorption test

The sorption test was conducted to further evaluate the impact of fertilization on the P sorption capacity of the separated organo-mineral complexes. Briefly, a 0.5 g sample of organo-mineral complexes was weighed into a 50-mL centrifuge tube and filled with 12.5 mL of P standard solutions with P concentrations of 0, 5, 10, 20, 40, 80, and 160 mg L^{-1}, which were configured with KH_2PO_4 in a 0.01 mol L^{-1} NaCl solution. One drop of chloroform was added into each tube to prevent microbial growth. Then, the mixtures in tubes were shaken (150 r min^{-1}) for 24 h at 25 °C and centrifuged (5 000 r min^{-1} for 10 min at 25 °C) to separate the soil solids and supernatant. After passing a 0.45-μm filter membrane, the P in the supernatant was determined by colorimetry as described above. According to the Langmuir isotherm equation (Langmuir, 1918), the isothermal sorption data were fitted as follows:

$$Q_{\mathrm{e}} = \frac{Q_{\mathrm{m}} K C_{\mathrm{e}}}{1 + K C_{\mathrm{e}}} \quad (1)$$

where Q_{e} (mg kg^{-1}) is the quantity of P adsorbed on soil organo-mineral complexes at equilibrium, C_{e} (mg L^{-1}) is the P concentration in solution at equilibrium, Q_{m} (mg kg^{-1}) is the maximum capacity of P sorption, and K is the equation constant associated with sorption binding energy.

Statistical analysis

All data for analysis of variance (ANOVA) conformed to normal distribution and variance homogeneity ($P > 0.05$) after the Shapiro-Wilk test and Levene test in SPSS version 23 (IBM Corp., USA). One-way ANOVA was carried out to compare the differences in the properties of organo-mineral complexes, MAOC fractions, P fractions, and P sorption parameters between fertilization treatments and between years, and *post-hoc* multiple comparison was performed using the least significant difference test at $P < 0.05$ level. Two-way ANOVA was used to identify the effects of year, treatment, and their interactions on the above properties. Redundancy analysis was used to explain the variations in P fractions using the vegan package in R version 4.2.2 (R Core Team, 2023), and hierarchical partitioning was performed to estimate the individual effect of each explanatory variable using the rdacca.cn package (Lai *et al*., 2022). OriginPro version 2023 (OriginLab Corporation, USA) was employed for Pearson's correlation analysis of variables and fitting the Langmuir isotherm equation to calculate the Q_{m} and K.

RESULTS

Properties of the organo-mineral complexes

Properties of the organo-mineral complexes were influenced by long-term fertilization (Table I). Compared to CK, the CF treatment significantly decreased the pH of the organo-mineral complexes by 19.1% in 2010 and 16.3% in 2018, while the CFS treatment maintained the pH. Both the CF and CFS treatments significantly increased total P content in the organo-mineral complexes by an average of 36.86% (33.3%–45.2%). Moreover, the contents of Fe_{o}, Fe_{p}, and Al_{p} were the highest in the CF treatment among the treatments in 2010 and 2018, whereas Ca_{ex} content was the highest in the CFS treatment.

MAOC fractions in the organo-mineral complexes

The contents of different MAOC fractions in the organo-mineral complexes were considerably impacted by long-term fertilization. Overall, total MAOC in the organo-mineral complexes accounted for approximately 44% of the initial OC in bulk soil (Fig. S1, see Supplementary Material for Fig. S1). Compared to CK, total MAOC content significantly increased by 13% and 41.3% in the CF and CFS treatments, respectively, in 2018 (Fig. 1). In 2010 and 2018, compared to CK, the CF treatment significantly decreased the content of K_2SO_4-OC while increasing the content of $Na_2B_4O_7$-OC, whereas the CFS treatment significantly increased the content of H_2SO_4-OC. Notably, the CFS treatment showed significantly higher contents of K_2SO_4-OC, $Na_4P_2O_7$-OC, H_2SO_4-OC, and humin in the organo-mineral complexes than the CF treatment in both 2010 and 2018.

P fractions in the organo-mineral complexes

Phosphorus in the organo-mineral complexes accounted for 29.2%–50.2% of the total P in bulk soil (Fig. S1). The content of each P fraction is shown in Fig. 2. Compared to CK, the CF treatment significantly increased resin-P_{i}, $NaHCO_3$-P_{i}, $NaHCO_3$-P_{o}, and NaOH-P_{i} contents by 207.5%–603.7% in 2010 and 2018. The CFS treatment significantly increased Dil. HCl-P_{i} and Con. HCl-P_{o} contents by 56.99%–78.50%, with a larger increase in Dil. HCl-P_{i} content than in Con. HCl-P_{o} content. The relative contribution of each P fraction to total P is shown in Fig. S2 (see Supplementary Material for Fig. S2). Compared to CK, the CF treatment increased the proportions of resin-P_{i}, $NaHCO_3$-P_{i}, $NaHCO_3$-P_{o}, NaOH-P_{i}, and NaOH-P_{o}, while the CFS treatment mainly increased the proportions of Dil. HCl-P_{i} and Con. HCl-P_{o}.

TABLE I

Selected properties[a)] of the organo-mineral complexes in soil samples under different fertilization treatments collected in 2010 and 2018 from a long-term field experiment established on a black soil in Gongzhuling, Jilin Province, Northeast China, in 1989

Year (Y)	Treatment (T)[b)]	pH	TP	Ca_{ex}	Mg_{ex}	Fe_o	Al_o	Fe_p	Al_p
			g kg^{-1}						
2010	CK	7.75 ± 0.37[c)]Aa[d)]	0.57 ± 0.03Ab	12.39 ± 2.35Aab	0.36 ± 0.11Aa	3.17 ± 0.10Ab	3.76 ± 0.36Aa	0.14 ± 0.03Ab	0.93 ± 0.07Ab
	CF	6.27 ± 0.11Ab	0.76 ± 0.00Ba	9.54 ± 0.20Ab	0.45 ± 0.12Aa	3.56 ± 0.14Aa	3.20 ± 0.06Bb	0.25 ± 0.02Ba	1.07 ± 0.07Ba
	CFS	7.84 ± 0.05Aa	0.77 ± 0.01Aa	13.10 ± 1.89Aa	0.28 ± 0.02Aa	2.70 ± 0.04Ac	3.37 ± 0.06Aab	0.12 ± 0.00Ab	0.86 ± 0.06Ab
2018	CK	7.35 ± 0.13Aa	0.62 ± 0.03Ab	8.57 ± 0.95Ab	0.32 ± 0.07Aa	2.25 ± 0.55Bb	2.98 ± 0.37Ab	0.17 ± 0.04Ab	0.96 ± 0.06Ab
	CF	6.15 ± 0.17Ab	0.90 ± 0.06Aa	6.76 ± 0.32Bb	0.36 ± 0.01Aa	3.92 ± 0.54Aa	4.05 ± 0.31Aa	0.37 ± 0.05Aa	1.31 ± 0.11Aa
	CFS	7.53 ± 0.25Aa	0.83 ± 0.04Aa	11.10 ± 1.30Aa	0.24 ± 0.02Bb	2.76 ± 0.38Ab	3.85 ± 0.40Aa	0.13 ± 0.01Ab	0.87 ± 0.03Ab
					Analysis of variance				
Y		*	***	**	ns[e)]	ns	ns	**	*
T		***	***	**	*	***	ns	***	***
Y × T		ns	ns	ns	ns	*	**	*	*

*, **, and ***Significant at $P < 0.05$, $P < 0.01$, and $P < 0.001$, respectively.

a) TP = total P; Ca_{ex} and Mg_{ex} = exchangeable Ca and Mg, respectively; Fe_o and Al_o = amorphous Fe and Al extracted by ammonium oxalate, respectively; Fe_p and Al_p = organically complexed Fe and Al extracted by $Na_4P_2O_7$, respectively.

b) CK = no fertilizer control; CF = chemical fertilizer; CFS = chemical fertilizer combined with straw addition.

c) Means ± standard deviations (n = 3).

d) Different lowercase letters within the same column indicate significant differences among different fertilization treatments for the same year at $P < 0.05$, and different uppercase letters within the same column indicate significant differences between different years for the same fertilization treatment at $P < 0.05$.

e) Not significant.

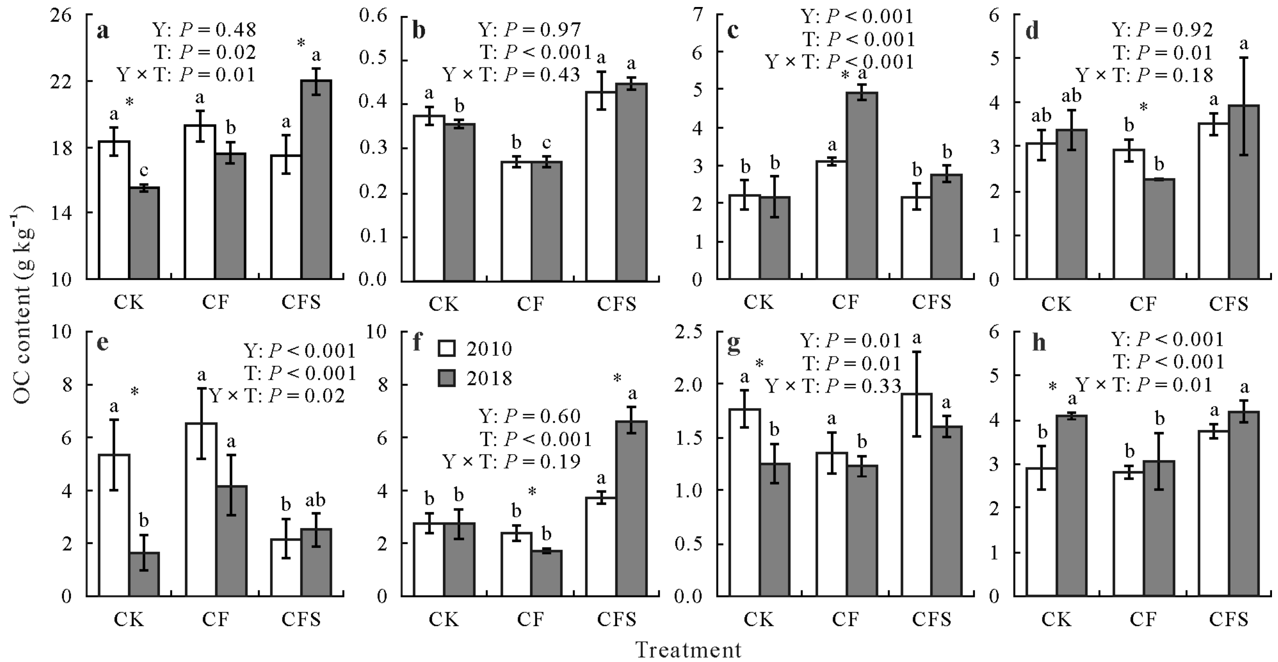

Fig. 1 Contents of total mineral-associated organic C (MAOC, a) and different MAOC fractions, including the remaining water-soluble organic C (OC) (extracted by K_2SO_4, K_2SO_4-OC, b), OC bound to minerals by weak linkages (extracted by $Na_2B_4O_7$, $Na_2B_4O_7$-OC, c), OC bound by cations (extracted by $Na_4P_2O_7$, $Na_4P_2O_7$-OC, d), OC extracted in massive quantities by NaOH (NaOH-OC, e), OC encapsulated by resistant carbonate (extracted by H_2SO_4 and NaOH, H_2SO_4-OC, f), OC stabilized by Fe (hydro)oxides (extracted by $Na_2S_2O_4$ and NaOH, $Na_2S_2O_4$-OC, g), and insoluble OC (humin, h), of the organo-mineral complexes in soil samples under different fertilization treatments collected in 2010 and 2018 from a long-term field experiment established on a black soil in Gongzhuling, Jilin Province, Northeast China, in 1989. Error bars are standard deviations of means (n = 3). Different letters indicate significant differences between different fertilization treatments for the same year at $P < 0.05$, and the asterisk * indicates significant differences between different years for the same fertilization treatment at $P < 0.05$. CK = no fertilizer control; CF = chemical fertilizer; CFS = chemical fertilizer combined with straw addition; Y = year; T = treatment.

P species in the organo-mineral complexes

Based on the linear combination fitting of P K-edge XANES spectra (Fig. 3), the species of P in the organo-mineral complexes were identified (Table II). The organo-mineral complexes were rich in P species, primarily $AlPO_4$, $Ca_3(PO_4)_2$, $Ca_5(PO_4)_3OH$, and inositol hexaphosphate. For CK, the dominant P species were mainly $AlPO_4$ and inosi-

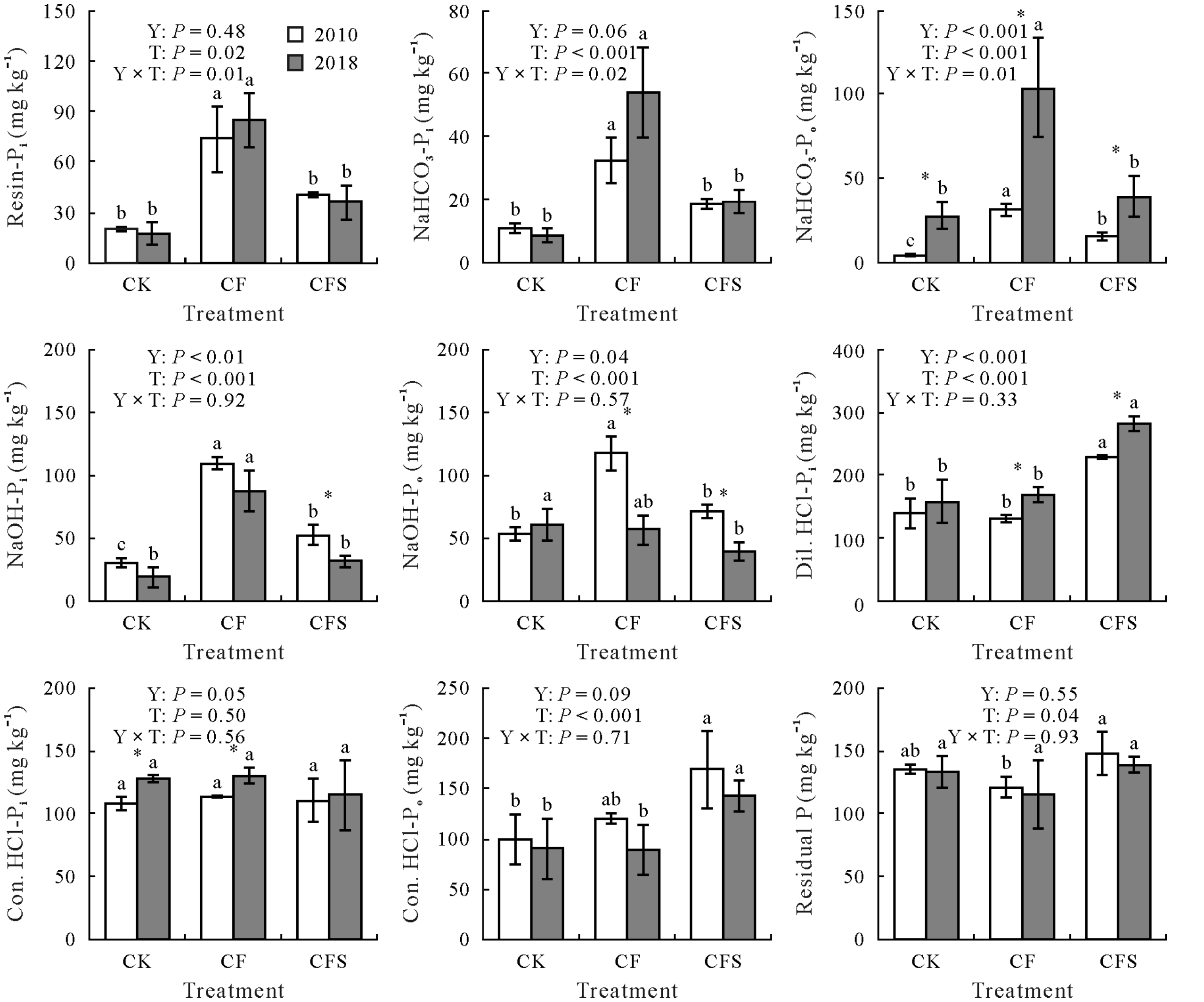

Fig. 2 Contents of different P fractions extracted sequentially by resin strips + deionized water (resin-inorganic P (P_i)), $NaHCO_3$ ($NaHCO_3$-P_i/organic P (P_o)), NaOH (NaOH-P_i/P_o), dilute HCl (Dil. HCl-P_i), concentrated HCl (Con. HCl-P_i/P_o), and H_2O_2 + H_2SO_4 (residual P) of the organo-mineral complexes in soil samples under different fertilization treatments collected in 2010 and 2018 from a long-term field experiment established on a black soil in Gongzhuling, Jilin Province, Northeast China, in 1989. Error bars are standard deviations of means (n = 3). Different letters indicate significant differences between different fertilization treatments for the same year at $P < 0.05$, and the asterisk * indicates significant differences between different years for the same fertilization treatment at $P < 0.05$. CK = no fertilizer control; CF = chemical fertilizer; CFS = chemical fertilizer combined with straw addition; Y = year; T = treatment.

tol hexaphosphate in 2010, whereas they were $Ca_3(PO_4)_2$ and $Ca_5(PO_4)_3OH$ in 2018. The dominant P species was $AlPO_4$ in the CF treatment, whereas the dominant P species was Ca-associated P, consisting mainly of $Ca_3(PO_4)_2$ and $Ca_5(PO_4)_3OH$, in the CFS treatment, and the proportions of these dominant P species increased over time.

P sorption on the organo-mineral complexes

The P sorption on the organo-mineral complexes was simulated using the Langmuir isotherm equation (Fig. 4), and the fitted parameters are summarized in Table III. Obviously, Q_m was notably higher in the CFS treatment than in CK and the CF treatment by 33.1% and 42.1%, respectively, in 2010. The Q_m in the CFS treatment was significantly lower in 2018 than in 2010, but remained 30.3% higher than in the CF treatment.

Relationships between P fractions, MAOC fractions, chemical properties, and P sorption capacity of the organo-mineral complexes

Redundancy analysis showed that 71% of the variations in P fractions could be explained by the chemical properties and MAOC fractions of the organo-mineral complexes (Fig. 5a). Some individual MAOC fractions ($Na_2B_4O_7$-OC, K_2SO_4-OC, and H_2SO_4-OC) and Fe/Al minerals (Fe_p, Fe_o, Al_p, and Al_o) had relatively significant effects on P fractions, with individual effect ranging from 9.4% to 13.3% (Fig. 5b). Further pairwise correlation analysis revealed that $Na_2B_4O_7$-

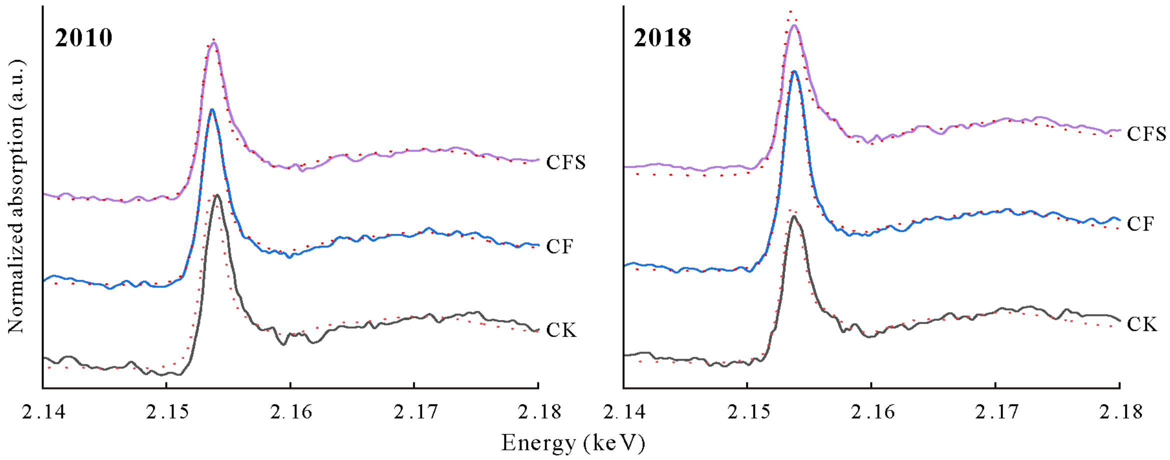

Fig. 3 Linear combination fitting of P K-edge X-ray absorption near-edge structure spectra of the organo-mineral complexes in soil samples under different fertilization treatments collected in 2010 and 2018 from a long-term field experiment established on a black soil in Gongzhuling, Jilin Province, Northeast China, in 1989. CK = no fertilizer control; CF = chemical fertilizer; CFS = chemical fertilizer combined with straw addition; a.u. = arbitrary units.

TABLE II

P species identified by the linear combination fitting of P K-edge X-ray absorption near-edge structure spectra in the organo-mineral complexes in soil samples under different fertilization treatments collected in 2010 and 2018 from a long-term field experiment established on a black soil in Gongzhuling, Jilin Province, Northeast China, in 1989

Year	Treatment[a)]	Proportion[b)]								R-factor[c)]
		$AlPO_4$	$FePO_4$	$CaHPO_4$	$Ca(H_2PO_4)_2$	$Ca_3(PO_4)_2$	$Ca_5(PO_4)_3OH$	Ca-P	IHP	
		%								
2010	CK	21.35	–[d)]	16.73	–	15.90	14.83	47.46	31.20	0.027
	CF	35.24	–	–	2.14	25.60	12.14	39.88	24.88	0.010
	CFS	22.12	–	4.56	–	32.61	22.35	59.52	18.36	0.010
2018	CK	18.72	9.74	12.69	–	23.33	35.51	71.53	–	0.030
	CF	42.84	5.31	–	–	17.55	9.01	26.56	25.29	0.008
	CFS	14.03	–	–	–	42.21	40.67	82.88	3.09	0.037

a) CK = no fertilizer control; CF = chemical fertilizer; CFS = chemical fertilizer combined with straw addition.
b) IHP = inositol hexakisphosphate; Ca-P = Ca-associated P, the sum of $CaHPO_4$, $Ca(H_2PO_4)_2$, $Ca_3(PO_4)_2$, and $Ca_5(PO_4)_3OH$.
c) R-factor indicates the goodness-of-fit of linear combination fitting.
d) Not detected.

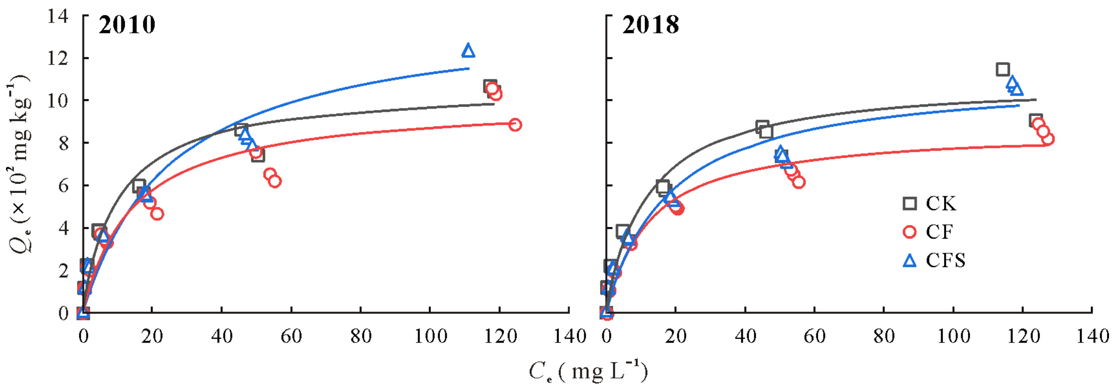

Fig. 4 Quantity of P adsorbed and P sorption isotherms of organo-mineral complexes in soil samples under different fertilization treatments collected in 2010 and 2018 from a long-term field experiment established on a black soil in Gongzhuling, Jilin Province, Northeast China, in 1989. CK = no fertilizer control; CF = chemical fertilizer; CFS = chemical fertilizer combined with straw addition; Q_e = quantity of P adsorbed on organo-mineral complexes at equilibrium; C_e = P concentration in solution at equilibrium.

OC had positive relationships with resin-P_i, $NaHCO_3$-P_i, $NaHCO_3$-P_o, NaOH-P_i, and NaOH-P_o, whereas K_2SO_4-OC, $Na_4P_2O_7$-OC, and H_2SO_4-OC were positively correlated with Dil. HCl-P_i and Q_m (Fig. 5c). The $Na_2S_2O_4$-OC and humin had positive relationships with residual P. Moreover, resin-P_i, $NaHCO_3$-P_i, NaOH-P_i, and NaOH-P_o were positively correlated with Fe_p, Fe_o, and Al_p, and Q_m had a positive relationship with Ca_{ex}.

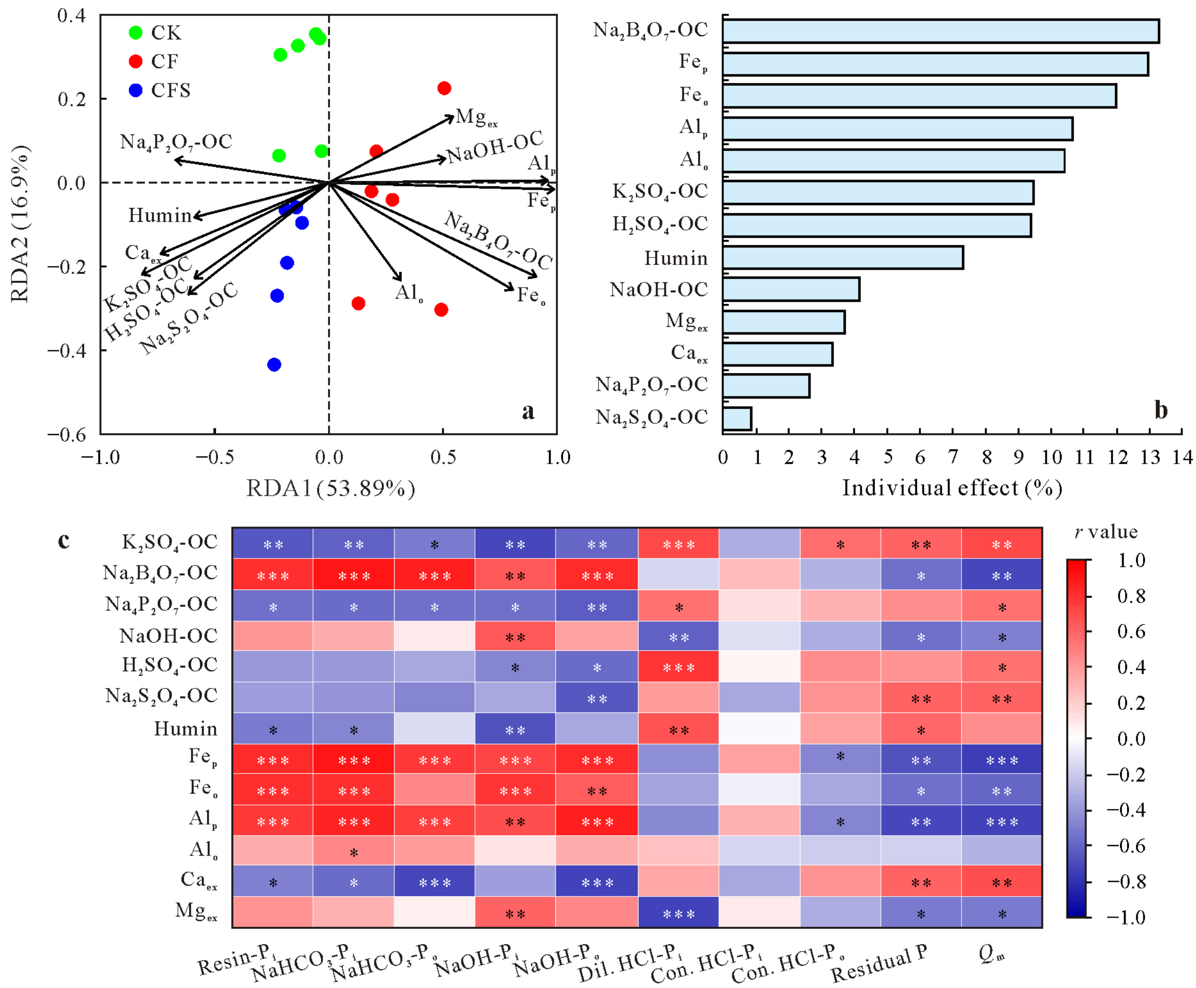

Fig. 5 Redundancy analysis (RDA) of the relationships between mineral-associated organic C (MAOC) fractions, chemical properties, and P fractions (a), individual effect of MAOC fractions and chemical properties on P fractions (b), Pearson's correlation analysis of P fractions, MAOC fractions, chemical properties, and P sorption capacity (c) of organo-mineral complexes in soil samples under different fertilization treatments collected in 2010 and 2018 from a long-term field experiment established on a black soil in Gongzhuling, Jilin Province, Northeast China, in 1989. Asterisks *, **, and *** indicate significant correlations at $P < 0.05$, $P < 0.01$, and $P < 0.001$, respectively. Q_m = maximum P sorption capacity; CK = no fertilizer control; CF = chemical fertilizer; CFS = chemical fertilizer combined with straw addition. See Fig. 1, Fig. 2, and Table I for the details of the MAOC fractions, P fractions, and chemical properties, respectively.

DISCUSSION

Effect of fertilization on the properties and MAOC fractions of organo-mineral complexes

Organo-mineral complexes, which are formed by the interaction of OM and minerals, are the prerequisite of soil OM preservation and aggregate structure development (Newcomb *et al*., 2017; Yu *et al*., 2017). As a result, due to the sequestration of P-containing OM and the aggregation of P-fixing substances, the organo-mineral complexes are more actively involved in P transformation and accumulation compared to silt and sand (Spohn, 2020; Takamoto *et al*., 2021). The organo-mineral complexes (< 20 μm) were abundant in the black soil, accounting for approximately 40% of the bulk soil mass (Fig. S1), and their properties were affected by fertilization. The CF treatment caused a significant reduction in soil pH and a significant increase in Fe_o, Fe_p, and Al_p contents in the organo-mineral complexes (Table I), similar to recent reports on other soil types (Du *et al*., 2022; Bai *et al*., 2023). This could be due to N leaching and base cation removal, leading to soil acidification (Lucas *et al*., 2011), which accelerates soil weathering and solubilization of soil minerals (Bunn *et al*., 2002; Meyer *et al*., 2021). Specifically, acidification promotes the solubilization of crystalline Fe and Al oxides, contributing to the formation of non-crystalline minerals (Guo *et al*., 2007). Straw substitution of 32% chemical N fertilizer (the CFS treatment) maintained soil pH and increased Ca_{ex} contents in the organo-mineral complexes (Table I), agreeing with the study of Wang *et al*. (2023) found that straw addition with proportions of N $\geqslant$ 20% had less effect on soil acidification compared to straw addition at proportions of < 20%. Moreover, the input of Ca derived from organic and mineral fertilizers promoted

TABLE III

Parameters of P sorption characteristics[a)] simulated using the Langmuir isotherm equation

Year (Y)	Treatment (T)[b)]	Q_m	K	R^2
		mg kg^{-1}		
2010	CK	1 069.16 ± 34.97[c)]Ab[d)]	0.10 ± 0.01Aa	0.95
	CF	1 001.15 ± 78.63Ab	0.07 ± 0.02Aa	0.93
	CFS	1 422.54 ± 7.19Aa	0.04 ± 0.00Bb	0.95
2018	CK	1 105.96 ± 153.98Aa	0.08 ± 0.01Aa	0.95
	CF	864.38 ± 43.94Ab	0.08 ± 0.01Aa	0.96
	CFS	1 126.37 ± 36.93Ba	0.06 ± 0.01Ab	0.95
		Analysis of variance		
Y		**	ns[e)]	
T		***	***	
Y×T		**	ns	

** and ***Significant at $P < 0.01$ and $P < 0.001$, respectively.

a) Q_m = maximum P sorption capacity; K = the equation constant associated with sorption binding energy.

b) CK = no fertilizer control; CF = chemical fertilizer; CFS = chemical fertilizer combined with straw addition.

c) Means ± standard deviations ($n = 3$).

d) Different lowercase letters within the same column indicate significant differences among different fertilization treatments for the same year at $P < 0.05$, and different uppercase letters within the same column indicate significant differences between different years for the same fertilization treatment at $P < 0.05$.

e) Not significant.

the accumulation of Ca_{ex} (Table I) (Chen M M *et al.*, 2021), which can buffer the changes in soil pH (Zhao *et al.*, 2023).

The total P in the organo-mineral complexes accounted for approximately 38.62% of the initial total P in the bulk soil (Fig. S1), indicating that the organo-mineral complexes are an important P reservoir. The content of total P in the organo-mineral complexes in the CF treatment increased with time (Table I). In the same experiment, a previous study showed that P input was higher than P output; and therefore, soil P was in surplus (Wu *et al.*, 2020). Surplus P can be adsorbed and fixed by soil minerals, resulting in soil P accumulation (MacDonald *et al.*, 2011; Zou *et al.*, 2022). The organo-mineral complexes were rich in minerals, facilitating the retention of surplus P. However, compared to the CF treatment, there was no significant difference in the total P content despite an annual increase of 6 kg ha^{-1} P in the CFS treatment, possibly because fresh OC input stimulated microbial turnover of P, which in turn may be transferred or consumed by the crops (Pu *et al.*, 2023). Overall, the accumulation of surplus P in the organo-mineral complexes may inhibit losses as free P and could also support the long-term P demand for maize.

After 29 years of fertilization, the CFS treatment resulted in greater promotion of MAOC compared to the CF treatment (Fig. 1), which was consistent with earlier findings from the same experiment (Mustafa *et al.*, 2022). Straw addition increases OC from microbial sources by stimulating microbial growth (Shang *et al.*, 2023). However, total MAOC content did not increase after 21 years of fertilization, suggesting that the impact of fertilization on MAOC is dependent on fertilization history. In the early stage of cultivation, the content of OC in bulk soil was similar among the different fertilization practices (Fig. S3, see Supplementary Material for Fig. S3) (Zhang *et al.*, 2010); however, the rate of OC promotion in the CFS treatment increased with time (Fig. S4). The change in total MAOC content may show similar patterns to OC in bulk soil, which could explain the difference observed between 2010 and 2018. Nonetheless, the MAOC fractions showed similar trends in 2010 and 2018, *i.e.*, the CF treatment decreased K_2SO_4-OC and increased $Na_2B_4O_7$-OC (Fig. 1). It is likely that N and P inputs increase C limitation and enhance biodegradation of high-labile C, such as dissolved OC (Li Z L *et al.*, 2023), which may be converted to more stable OC by weak sorption of soil minerals at lower soil pH. The CFS treatment significantly increased the H_2SO_4-OC (Fig. 1), which could be due to the abundance of Ca-bound and encapsulated OC by Ca bridging at higher soil pH (Chen *et al.*, 2014; Rowley *et al.*, 2018). Additionally, the changes in the MAOC fractions under the fertilization treatments (CF and CFS) were almost continuously enhanced from 2010 to 2018, whereby some significant differences occurred in different years under the same treatment (Fig. 1). However, for CK, except for $Na_4P_2O_7$-OC and humin, the contents of other MAOC fractions were reduced to varying degrees from 2010 to 2018 (Fig. 1), which could be due to the reduced microbial contribution to MAOC caused by climate warming (Chen *et al.*, 2023). Chemical fertilizer and straw addition counteracted this change, possibly by decreasing the dependency of the organisms released from soil OM decomposition *via* nutrient supply (Liu *et al.*, 2023), as well as promoting the mineralogical capacity of OC *via* increasing extractable minerals (Table I).

Effect of fertilization on P fractions in the organo-mineral complexes

The CF treatment over 21 years increased the contents of resin-P_i, $NaHCO_3$-P_i, $NaHCO_3$-P_o, and NaOH-P_i in the organo-mineral complexes and their relative contributions to total P (Figs. 2 and S2). According to Tiessen and Moir (1993), resin-P_i is freely exchangeable P_i; $NaHCO_3$-P_i is plant-available since the chemical changes introduced are minor and somewhat representative of root action; correspondingly, $NaHCO_3$-P_o is likely to be utilized by microorganisms; and NaOH-P_i represents a continuum of Fe/Al-associated P extractable with increasing pH, indicating that this pool exhibits higher solubility in the black soil relative to the soil with lower pH. These P fractions have higher plant availability and are usually classified as labile or moderately labile P (Cross and Schlesinger, 1995; Gatiboni *et* *al*., 2021). According to the XANES results, the proportion of Al-associated P ($AlPO_4$) increased significantly in the CF treatment (Table II), suggesting that the increased labile/moderately labile P is mainly associated with Al. This is supported by Wang *et al*. (2022a), who found that Al-associated P is a potential pool of available P in the black soil. Although almost no Fe-associated P ($FePO_4$) was detected, this does not mean that it is absent from the soil, because the accuracy of XANES-linear combination fitting depends on various factors such as the content of P species (Beauchemin *et al*., 2003; Kizewski *et al*., 2011). However, based on the pH dependence of P fixation, *i.e.*, the predominance of P fixation by Al under weakly acidic conditions (Barrow, 2017), our results are sufficiently plausible. In this experiment, triple superphosphate was used as P fertilizer, but the increase in Ca-associated P was not observed, which indicated that acidification promoted the solubilization of Ca-associated P (Andersson *et al*., 2016). Meanwhile, soil acidification also provides additional P sorption sites by enhancing the solubilization of soil Al (Table I), and solubilized P can be secondary sorbed by Al to form Al-associated P (Meyer *et al*., 2021).

The CFS treatment increased the content and proportion of Dil. HCl-P_i (Figs. 2 and S2), which was Ca-associated P (Tiessen and Moir, 1993). The XANES results further revealed that the molecular species of increased Ca-associated P were $Ca_3(PO_4)_2$ and $Ca_5(PO_4)_3OH$ (Table II). The soil pH was weakly alkaline in the CFS treatment (Table I), which contributed to the sorption and precipitation of Ca-associated P (Tunesi *et al*., 1999; Barrow, 2017). The CFS treatment also notably increased the content of Con. HCl-P_o in the organo-mineral complexes (Fig. 2), similar to the results of a recent study that the return of maize straw increased highly resistant P_o content in the 0–20 cm topsoil (Cao *et al*., 2021). Straw enhanced the accumulation of soil P_o, such as P monoesters (Li *et al*., 2019), which can be coprecipitated with soil minerals to form stabilized P_o (Wang *et al*., 2017). Overall, the accumulation of all P_i forms in soil was pH-dependent, regardless of fertilization practices, whereas P_o may depend on C input.

Relationships between P forms and MAOC fractions in the organo-mineral complexes

In this study, corn yield showed no significant difference between the CF and CFS treatments (Fig. S4, see Supplementary Material for Fig. S4), implying that maize uptake of P barely explained the variations in soil P. We found that the chemical properties and MAOC fractions of organo-mineral complexes explained 71% of the variations in P fractions (Fig. 5a). The MAOC fractions, especially $Na_2B_4O_7$-OC, K_2SO_4-OC, and H_2SO_4-OC, and the Fe/Al minerals had an individual effect on P fraction variations, ranging from 9.4% to 13.3% (Fig. 5b), suggesting that these properties of organo-mineral complexes were the contributing factors and predictors of the P fractions. Previous studies have also found that soil properties, especially metal minerals and OM, are important factors influencing P pools (Fan *et al*., 2019; Chen S *et al*., 2021) and that each P fraction may have specific drivers (Deiss *et al*., 2018). Furthermore, it was also previously found that OM in bulk soil is the main factor affecting changes in P fractions (Wang *et al*., 2022b; Zhang N Y *et al*., 2022); however, a deeper understanding of this effect remains unclear. In this study, almost all labile and moderately P fractions in the organo-mineral complexes were positively correlated with $Na_2B_4O_7$-OC, Fe_p, Fe_o, and Al_p (Fig. 5c), and these P fractions and chemical properties were dominant in the CF treatment. Despite the significant increase in total P (Table I), the Q_m of organo-mineral complexes after 21 years of chemical fertilizer application was similar to that of CK (Table III), implying that more sorption sites were created to compensate for the sites occupied by earlier P. This was supported by our and other research findings that chemical fertilizer application increased the P sorption sites, such as amorphous Fe/Al (Table I) (Abdala *et al*., 2015). The amorphous Fe/Al can be adsorbed by OM, thus preventing the formation of Fe/Al-P co-precipitates (Chen and Thompson, 2018; Ge *et al*., 2020). Moreover, Fe/Al can exist as a cationic bridge between P and OM to form a ternary mixture of OM-Fe/Al-P that maintains the availability of P (Gerke, 2010; Takamoto *et al*., 2021). Our results further supported that liable P fractions in the organo-mineral complexes were more likely to be associated with Al. Therefore, the potential mechanism may be that MAOC bound to Al minerals by weak linkages promotes the retention of highly labile P fractions in weakly acidic environments.

The Dil. HCl-P_i and Q_m of organo-mineral complexes were significantly positively correlated with K_2SO_4-OC, $Na_4P_2O_7$-OC, and H_2SO_4-OC, and Q_m was positively correlated with Ca_{ex} (Fig. 5c). The Dil. HCl-P_i, Q_m, and these MAOC fractions were dominant in the CFS treatment. It has been reported that the Q_m of black soil at another site increased with increasing OM content (Yang *et al*., 2019). Therefore, we suggested that OM promoted the sorption and retention of P in weakly alkaline conditions *via* the association with Ca. Similar to Fe/Al, OM association with amorphous Ca minerals can adsorb P to form ternary mixtures of OM-Ca-P (Ge *et al*., 2020; Li *et al*., 2021). These ternary mixtures can inhibit the precipitation of Ca-P in a short period (Sindelar *et al*., 2015; Ge *et al*., 2020); however, the increase in the proportion of $Ca_3(PO_4)_2$ and $Ca_5(PO_4)_3OH$ in the CFS treatment (Table II) suggested that after the mobilization of OM, this accumulated OM-Ca-P might transform to the more stable Ca-P. Therefore, regardless of whether chemical fertilizer was applied or straw was added, MAOC could promote the accumulation and transformation of the corresponding P fractions or forms, and these processes were mineral- and pH-dependent.

The sequestration of soil OM is essential for peak carbon emissions and carbon neutrality (Li M *et al.*, 2023), as well as soil fertility and health (Li X *et al.*, 2023). Statistically, global MAOC in soil surface accounts for only 42% of the mineralogical capacity (Georgiou *et al.*, 2022), implying a huge potential for OC sequestration. The OC sequestration enhances soil functioning and crop productivity by promoting the formation of soil macro-aggregates (Tian *et al.*, 2022). Meanwhile, soil aggregation can reduce P loss *via* the occlusion of P into aggregates (Garland *et al.*, 2018). In this study, the application of chemical fertilizer increased the mineralogical capacity due to the increase in extractable Fe and Al, but the MAOC content was limited by the C input. The organo-mineral complexes promoted the storage of Ca-related C in the CFS treatment, because of richer Ca and higher pH compared to the CF treatment. Regardless of the fertilization practices, the presence of MAOC associated with metal minerals enhanced the accumulation of P related to those metal minerals. For the CFS treatment, the organo-mineral complexes exhibited higher P adsorption capacity and had more stable P forms, suggesting higher P retention capacity and fewer P loss. A combination of corn yield, MAOC sequestration, and P retention suggests that CFS is better suited for the black soil. This study was carried out under the same climatic conditions and a single cropping system, and the effects of additional factors such as cropping system, tillage practices, and climatic conditions on OC, P pools, and their interactions in the organo-mineral complexes still need to be further explored.

CONCLUSIONS

The MAOC fractions in the organo-mineral complexes of the black soil were affected by fertilization. Compared to CK, the CF treatment significantly reduced soil pH and increased $Na_2B_4O_7$-OC. The CFS treatment had higher soil pH and MAOC fractions (K_2SO_4-OC, $Na_4P_2O_7$-OC, H_2SO_4-OC, and humin) than the CF treatment. The CF and CFS treatments significantly increased total P content in the organo-mineral complexes. The CF treatment mainly increased highly labile P fractions, which may be mainly associated with Al, while the CFS treatment increased moderately labile Ca-associated P and stable P_o. In addition, the CFS treatment also increased the Q_m of the organo-mineral complexes. These results indicated that MAOC promoted the retention of highly labile P *via* the association with Al in the CF treatment, while MAOC enhanced the P sorption capacity and the accumulation of Ca-associated P *via* the association with Ca ions in the CFS treatment. Our findings revealed the synergistic effects and mechanisms between MAOC and P accumulation and provided a basis for regulating P with OC to achieve sustainable P utilization in agriculture.

DECLARATION OF COMPETING INTEREST

The authors declare that they have no known competing financial interests or personal relationships that could have appeared to influence the work reported in this paper.

ACKNOWLEDGEMENTS

This work was supported by the National Key Research and Development Program of China (No. 2022YFD1500101) and the National Natural Science Foundation of China (No. 41977103). We thank all the staff at the National Long-term Location Monitoring Base of Black Soil Fertility and Fertilizer Efficiency, Jilin Academy of Agricultural Sciences, China. We also thank Drs. Qiong Xiao, Shuai Zhang, and Jun Wang from the Institute of Agricultural Resources and Regional Planning, Chinese Academy of Agricultural Sciences, for their insightful suggestions and writing assistance.

SUPPLEMENTARY MATERIAL

Supplementary material for this article can be found in the online version.

REFERENCES

Abdala D B, da Silva I R, Vergütz L, Sparks D L. 2015. Long-term manure application effects on phosphorus speciation, kinetics and distribution in highly weathered agricultural soils. *Chemosphere*. **119**: 504–514.

Andersson K O, Tighe M K, Guppy C N, Milham P J, McLaren T I. 2016. The release of phosphorus in alkaline vertic soils as influenced by pH and by anion and cation sinks. *Geoderma*. **264**: 17–27.

Ando K, Yamaguchi N, Kasuya M, Oga T, Ohashi Y, Taki K. 2022. Long-term (nearly a century) effects of fertilizer, lime and rice straw compost application on active aluminum and iron and available phosphorus in paddy fields. *Geoderma*. **424**: 115992.

Audette Y, O'Halloran I P, Voroney R P. 2016. Kinetics of phosphorus forms applied as inorganic and organic amendments to a calcareous soil. *Geoderma*. **262**: 119–124.

Bai S S, Tan J F, Zhang Z Y, Wei M, Zhang H M, Jiang X Q. 2023. Phosphorus speciation and colloidal phosphorus responses to short-term cessation of fertilization in a lime concretion black soil. *Pedosphere*. **33**: 948–959.

Barrow N J. 2017. The effects of pH on phosphate uptake from the soil. *Plant Soil*. **410**: 401–410.

Beauchemin S, Hesterberg D, Chou J, Beauchemin M, Simard R R, Sayers D E. 2003. Speciation of phosphorus in phosphorus-enriched agricultural soils using X-ray absorption near-edge structure spectroscopy and chemical fractionation. *J Environ Qual*. **32**: 1809–1819.

Bunn R A, Magelky R D, Ryan J N, Elimelech M. 2002. Mobilization of natural colloids from an iron oxide-coated sand aquifer: Effect of pH and ionic strength. *Environ Sci Technol*. **36**: 314–322.

Cao D Y, Lan Y, Sun Q, Yang X, Chen W F, Meng J, Wang D, Li N. 2021. Maize straw and its biochar affect phosphorus distribution in soil aggregates and are beneficial for improving phosphorus availability along the soil profile. *Eur J Soil Sci*. **72**: 2165–2179.

Cao N, Zhi M L, Zhao W Q, Pang J Y, Hu W, Zhou Z G, Meng Y L. 2022. Straw retention combined with phosphorus fertilizer promotes soil phosphorus availability by enhancing soil P-related enzymes and the abundance of *phoC* and *phoD* genes. *Soil Tillage Res*. **220**105390.

Chen C M, Dynes J J, Wang J, Karunakaran C, Sparks D L. 2014. Soft X-ray spectromicroscopy study of mineral-organic matter associations in pasture soil clay fractions. *Environ Sci Technol*. **48**: 6678–6686.

Chen C M, Thompson A. 2018. Ferrous iron oxidation under varying pO_2 levels: The effect of Fe(III)/Al(III) oxide minerals and organic matter. *Environ Sci Technol*. **52**: 597–606.

Chen M M, Zhang S R, Liu L, Wu L P, Ding X D. 2021. Combined organic amendments and mineral fertilizer application increase rice yield by improving soil structure, P availability and root growth in saline-alkaline soil. *Soil Tillage Res*. **212**: 105060.

Chen S, Cade-Menun B J, Bainard L D, St. Luce M, Hu Y F, Chen Q. 2021. The influence of long-term N and P fertilization on soil P forms and cycling in a wheat/fallow cropping system. *Geoderma*. **404**: 115274.

Chen Y, Han M G, Yuan X, Zhou H K, Zhao X Q, Schimel J P, Zhu B. 2023. Long-term warming reduces surface soil organic carbon by reducing mineral-associated carbon rather than "free" particulate carbon. *Soil Biol Biochem*. **177**: 108905.

Cordell D, Drangert J O, White S. 2009. The story of phosphorus: Global food security and food for thought. *Glob Environ Chang*. **19**: 292–305.

Cross A F, Schlesinger W H. 1995. A literature review and evaluation of the Hedley fractionation: Applications to the biogeochemical cycle of soil phosphorus in natural ecosystems. *Geoderma*. **64**: 197–214.

Cui J W, Zhang S, Wang X Y, Xu X P, Ai C, Liang G Q, Zhu P, Zhou W. 2022. Enzymatic stoichiometry reveals phosphorus limitation-induced changes in the soil bacterial communities and element cycling: Evidence from a long-term field experiment. *Geoderma*. **426**: 116124.

de Oliveira L E Z, de Souza Nunes R, de Figueiredo C C, Rein T A. 2022. Spatial distribution of soil phosphorus fractions in a clayey oxisol submitted to long-term phosphate fertilization strategies. *Geoderma*. **418**: 115847.

Deiss L, de Moraes A, Maire V. 2018. Environmental drivers of soil phosphorus composition in natural ecosystems. *Biogeosciences*. **15**: 4575–4592.

Du J X, Liu K L, Huang J, Han T F, Zhang L, Anthonio C K, Shah A, Khan M N, Qaswar M, Abbas M, Huang Q H, Xu Y M, Zhang H M. 2022. Organic carbon distribution and soil aggregate stability in response to long-term phosphorus addition in different land-use types. *Soil Tillage Res*. **215**: 105195.

Fan Y X, Zhong X J, Lin F, Liu C C, Yang L M, Wang M H, Chen G S, Chen Y, Yang Y S. 2019. Responses of soil phosphorus fractions after nitrogen addition in a subtropical forest ecosystem: Insights from decreased Fe and Al oxides and increased plant roots. *Geoderma*. **337**: 246–255.

Fink J R, Inda A V, Tiecher T, Barrón V. 2016. Iron oxides and organic matter on soil phosphorus availability. *Ciênc Agrotec*. **40**: 369–379.

Garland G, Bünemann E K, Oberson A, Frossard E, Snapp S, Chikowo R, Six J. 2018. Phosphorus cycling within soil aggregate fractions of a highly weathered tropical soil: A conceptual model. *Soil Biol Biochem*. **116**, 91–98.

Gatiboni L C, Schmitt D E, Tiecher T, Veloso M G, dos Santos D R, Kaminski J, Brunetto G. 2021. Plant uptake of legacy phosphorus from soils without P fertilization. *Nutr Cycl Agroecosyst*. **119**: 139–151.

Ge X F, Wang L J, Zhang W J, Putnis C V. 2020. Molecular understanding of humic acid-limited phosphate precipitation and transformation. *Environ Sci Technol*. **54**: 207–215.

Georgiou K, Jackson R B, Vindušková O, Abramoff R Z, Ahlström A, Feng W T, Harden J W, Pellegrini A F A, Polley H W, Soong J L, Riley W J, Torn M S. 2022. Global stocks and capacity of mineral-associated soil organic carbon. *Nat Commun*. **13**: 3797.

Gerke J. 2010. Humic (organic matter)-Al(Fe)-phosphate complexes: An underestimated phosphate form in soils and source of plant-available phosphate. *Soil Sci*. **175**: 417–425.

Guo X M, Wu H H, Luo M, He G P. 2007. The morphological change of Fe/Al-oxide minerals in red soils in the process of acidification and its environmental significance. *Acta Petrol Mineral* (in Chinese). **26**: 515–521.

Jindo K, Audette Y, Olivares F L, Canellas L P, Smith D S, Voroney R P. 2023. Biotic and abiotic effects of soil organic matter on the phytoavailable phosphorus in soils: A review. *Chem Biol Technol Agric*. **10**: 29.

Kang J, Hesterberg D, Osmond D L. 2009. Soil organic matter effects on phosphorus sorption: A path analysis. *Soil Sci Soc Am J*. **73**: 360–366.

Kizewski F, Liu Y T, Morris A, Hesterberg D. 2011. Spectroscopic approaches for phosphorus speciation in soils and other environmental systems. *J Environ Qual*. **40**: 751–766.

Lai J S, Zou Y, Zhang J L, Peres-Neto P R. 2022. Generalizing hierarchical and variation partitioning in multiple regression and canonical analyses using the rdacca.hp R package. *Methods Ecol Evol*. **13**: 782–788.

Langmuir I. 1918. The adsorption of gases on plane surfaces of glass, mica and platinum. *J Am Chem Soc*. **40**: 1361–1403.

Li F Y, Liang X Q, Zhang H F, Tian G M. 2019. The influence of no-till coupled with straw return on soil phosphorus speciation in a two-year rice-fallow practice. *Soil Tillage Res*. **195**: 104389.

Li F Y, Zhang Q, Klumpp E, Bol R, Nischwitz V, Ge Z, Liang X Q. 2021. Organic carbon linkage with soil colloidal phosphorus at regional and field scales: Insights from size fractionation of fine particles. *Environ Sci Technol*. **55**: 5815–5825.

Li K J, Bi Q F, Liu X P, Wang H B, Sun C L, Zhu Y G, Lin X Y. 2022. Unveiling the role of dissolved organic matter on phosphorus sorption and availability in a 5-year manure amended paddy soil. *Sci Total Environ*. **838**: 155892.

Li M, Peng J Y, Lu Z X, Zhu P Y. 2023. Research progress on carbon sources and sinks of farmland ecosystems. *Resour Environ Sustain*. **11**: 100099.

Li X, Qiao L, Huang Y P, Li D C, Xu M G, Ge T D, Meersmans J, Zhang W J. 2023. Manuring improves soil health by sustaining multifunction at relatively high levels in subtropical area. *Agric Ecosyst Environ*. **353**: 108539.

Li Z L, Xu W J, Kang L Y, Kuzyakov Y, Chen L Y, He M, Liu F T, Zhang D Y, Zhou W, Liu X N, Yang Y H. 2023. Accelerated organic matter decomposition in thermokarst lakes upon carbon and phosphorus inputs. *Glob Chang Biol*. **29**: 6367–6382.

Liu J, Yang J J, Cade-Menun B J, Hu Y F, Li J M, Peng C, Ma Y B. 2017. Molecular speciation and transformation of soil legacy phosphorus with and without long-term phosphorus fertilization: Insights from bulk and microprobe spectroscopy. *Sci Rep*. **7**: 15354.

Liu J, Sui P, Cade-Menun B J, Hu Y F, Yang J J, Huang S M, Ma Y B. 2019. Molecular-level understanding of phosphorus transformation with long-term phosphorus addition and depletion in an alkaline soil. *Geoderma*. **353**: 116–124.

Liu Y H, Li C, Cai G, Sauheitl L, Xiao M L, Shibistova O, Ge T D, Guggenberger G. 2023. Meta-analysis on the effects of types and levels of N, P, and K fertilization on organic carbon in cropland soils. *Geoderma*. **437**: 116580.

Lopez-Sangil L, Rovira P. 2013. Sequential chemical extractions of the mineral-associated soil organic matter: An integrated approach for the fractionation of organo-mineral complexes. *Soil Biol Biochem*. **62**: 57–67.

Lu R K. 2000. Analytical Methods for Soil and Agricultural Chemistry (in Chinese). Agricultural Science and Technology Press, Beijing.

Lucas R W, Klaminder J, Futter M N, Bishop K H, Egnell G, Laudon H, Högberg P. 2011. A meta-analysis of the effects of nitrogen additions on base cations: Implications for plants, soils, and streams. *Forest Ecol Manage*. **262**: 95–104.

MacDonald G K, Bennett E M, Potter P A, Ramankutty N. 2011. Agronomic phosphorus imbalances across the world's croplands. *Proc Acad Natl Sci USA*. **108**: 3086–3091.

McKeague J A, Day J H. 1966. Dithionite- and oxalate-extractable Fe and Al as aids in differentiating various classes of soils. *Can J Soil Sci*. **46**: 13–22.

Meyer G, Bell M J, Lombi E, Doolette C L, Brunetti G, Novotny E H, Klysubun W, Zhang Y Q, Kopittke P M. 2021. Phosphorus speciation in the fertosphere of highly concentrated fertilizer bands. *Geoderma*. **403**: 115208.

Mikutta R, Kleber M, Torn M S, Jahn R. 2006. Stabilization of soil organic matter: Association with minerals or chemical recalcitrance? *Biogeochemistry*. **77**: 25–56.

Mogollón J M, Beusen A H W, van Grinsven H J M, Westhoek H, Bouwman A F. 2018. Future agricultural phosphorus demand according to the shared socioeconomic pathways. *Glob Environ Chang*. **50**: 149–163.

Murphy J, Riley J P. 1962. A modified single solution method for the determination of phosphate in natural waters. *Anal Chim Acta*. **27**: 31–36.

Mustafa A, Frouz J, Naveed M, Zhu P, Sun N, Xu M G, Núñez-Delgado A. 2022. Stability of soil organic carbon under long-term fertilization: Results from ^{13}C NMR analysis and laboratory incubation. *Environ Res*. **205**: 112476.

Newcomb C J, Qafoku N P, Grate J W, Bailey V L, De Yoreo J J. 2017. Developing a molecular picture of soil organic matter-mineral interactions by quantifying organo-mineral binding. *Nat Commun*. **8**: 396.

Pu J H, Jiang N, Zhang Y L, Guo L L, Huang W J, Chen L J. 2023. Effects of various straw incorporation strategies on soil phosphorus fractions and transformations. *Glob Chang Biol*. **15**: 88–98.

Rowley M C, Grand S, Verrecchia É P. 2018. Calcium-mediated stabilisation of soil organic carbon. *Biogeochemistry*. **137**: 27–49.

Sayer E J, Lopez-Sangil L, Crawford J A, Bréchet L M, Birkett A J, Baxendale C, Castro B, Rodtassana C, Garnett M H, Weiss L, Schmidt M W I. 2019. Tropical forest soil carbon stocks do not increase despite 15 years of doubled litter inputs. *Sci Rep*. **9**: 18030.

Schmidt M W I, Torn M S, Abiven S, Dittmar T, Guggenberger G, Janssens I A, Kleber M, Kögel-Knabner I, Lehmann J, Manning D A C, Nannipieri P, Rasse D P, Weiner S, Trumbore S E. 2011. Persistence of soil organic matter as an ecosystem property. *Nature*. **478**: 49–56.

Shang W H, Razavi B S, Yao S H, Hao C K, Kuzyakov Y, Blagodatskaya E, Tian J. 2023. Contrasting mechanisms of nutrient mobilization in rhizosphere hotspots driven by straw and biochar amendment. *Soil Biol Biochem*. **187**: 109212.

Shen J B, Wang L Y, Jiao X Q, Meng F L, Zhang L, Feng G, Zhang J L, Yuan L X, Ma L, Hou Y, Zhang T, Zhang W F, Li G H, Zhang K, Zhang F S. 2019. Innovations of phosphorus sustainability: Implications for the whole chain. *Front Agric Sci Eng*. **6**: 321–331.

Sindelar H R, Brown M T, Boyer T H. 2015. Effects of natural organic matter on calcium and phosphorus co-precipitation. *Chemosphere*. **138**: 218–224.

Soon Y K, Abboud S. 1991. A comparison of some methods for soil organic carbon determination. *Commun Soil Sci Plant Anal*. **22**: 943–954.

Spohn M. 2020. Phosphorus and carbon in soil particle size fractions: A synthesis. *Biogeochemistry*. **147**: 225–242.

Takamoto A, Hashimoto Y, Asano M, Noguchi K, Wagai R. 2021. Distribution and chemical species of phosphorus across density fractions in andisols of contrasting mineralogy. *Geoderma*. **395**: 115080.

Tian S Y, Zhu B J, Yin R, Wang M W, Jiang Y J, Zhang C Z, Li D M, Chen X Y, Kardol P, Liu M Q. 2022. Organic fertilization promotes crop productivity through changes in soil aggregation. *Soil Biol Biochem*. **165**: 108533.

Tiessen H, Moir J O. 1993. Characterization of available P by sequential extraction. *In* Carter M R, Gregorich E G (eds) Soil Sampling and Methods of Analysis. Lewis Publishers, Boca Raton. pp. 75–86.

Tunesi S, Poggi V, Gessa C. 1999. Phosphate adsorption and precipitation in calcareous soils: The role of calcium ions in solution and carbonate minerals. *Nutr Cycl Agroecosyst*. **53**: 219–227.

Wang Q, Qin Z H, Zhang W W, Chen Y H, Zhu P, Peng C, Wang L, Zhang S X, Colinet G. 2022a. Effect of long-term fertilization on phosphorus fractions in different soil layers and their quantitative relationships with soil properties. *J Integr Agric*. **21**: 2720–2733.

Wang Q, Zhang N Y, Chen Y H, Qin Z H, Jin Y W, Zhu P, Peng C, Colinet G, Zhang S X, Liu J. 2022b. The phosphorus availability in mollisol is determined by inorganic phosphorus fraction under long-term different phosphorus fertilization regimes. *Agronomy*. **12**: 2364.

Wang X M, Hu Y F, Tang Y D, Yang P, Feng X H, Xu W Q, Zhu M Q. 2017. Phosphate and phytate adsorption and precipitation on ferrihydrite surfaces. *Environ Sci Nano*. **4**: 2193–2204.

Wang Z, Tao T T, Wang H, Chen J, Small G E, Johnson D, Chen J H, Zhang Y J, Zhu Q C, Zhang S M, Song Y T, Kattge J, Guo P, Sun X. 2023. Forms of nitrogen inputs regulate the intensity of soil acidification. *Glob Chang Biol*. **29**: 4044–4055.

Wu Q H, Zhang S X, Feng G, Zhu P, Huang S M, Wang B R, Xu M G. 2020. Determining the optimum range of soil Olsen P for high P use efficiency, crop yield, and soil fertility in three typical cropland soils. *Pedosphere*. **30**: 832–843.

Wu Z, Li J C, Sun Y X, Peñuelas J, Huang J L, Sardans J, Jiang Q S, Finlay J C, Britten G L, Follows M J, Gao W, Qin B Q, Ni J R, Huo S L, Liu Y. 2022. Imbalance of global nutrient cycles exacerbated by the greater retention of phosphorus over nitrogen in lakes. *Nat Geosci*. **15**: 464–468.

Yan Z J, Chen S, Dari B, Sihi D, Chen Q. 2018. Phosphorus transformation response to soil properties changes induced by manure application in a calcareous soil. *Geoderma*. **322**: 163–171.

Yang W L, Xiang W, Bao Z Y, Huang C L, Ma M, Lu X Z, Yao L Y, Wang Y. 2022. Phosphorus sorption capacity of various iron-organic matter associations in peat soils. *Environ Sci Pollut Res*. **29**: 77580–77592.

Yang X Y, Chen X W, Yang X T. 2019. Effect of organic matter on phosphorus adsorption and desorption in a black soil from Northeast China. *Soil Tillage Res*. **187**: 85–91.

Yu G H, Xiao J, Hu S J, Polizzotto M L, Zhao F J, McGrath S P, Li H, Ran W, Shen Q R. 2017. Mineral availability as a key regulator of soil carbon storage. *Environ Sci Technol*. **51**: 4960–4969.

Zhang N Y, Wang Q, Zhan X Y, Wu Q H, Huang S M, Zhu P, Yang X Y, Zhang S X. 2022. Characteristics of inorganic phosphorus fractions and their correlations with soil properties in three non-acidic soils. *J Integr Agric*. **21**: 3626–3636.

Zhang W J, Wang X J, Xu M G, Huang S M, Liu H, Peng C. 2010. Soil organic carbon dynamics under long-term fertilizations in arable land of northern China. *Biogeosciences*. **7**: 409–425.

Zhang Y J, Gao W, Luan H A, Tang J W, Li R N, Li M Y, Zhang H Z, Huang S W. 2022. Long-term straw addition promotes moderately labile phosphorus formation, decreasing phosphorus downward migration and loss in greenhouse vegetable soil. *J Integr Agric*. **21**: 2734–2749.

Zhao G S, Huang Q B, Zhu Y N, Xu Y L, Pu Z G. 2023. Simulation of the buffering process of karst soil on sulfuric acid rain and the characteristic of $\delta^{13}C_{DIC}$ and the carbon sink flux in Guilin City, Southwest China. *Environ Earth Sci*. **82**: 296.

Zheng X H, Oba B T, Wang H, Zhang B, Shu C Q, Song Y, Fu J F, Liu S J, Zhang Y X, Dai N, Song D, Ding H. 2023. Revealing the potential of organo-mineral complexes in agricultural application using bibliometrics. *J Clean Prod*. **401**: 136728.

Zou T, Zhang X, Davidson E A. 2022. Global trends of cropland phosphorus use and sustainability challenges. *Nature*. **611**: 81–87.